How the biotin-streptavidin interaction was made even stronger: investigation via crystallography and a chimeric tetramer

Claire E Chivers, Apurba L Koner, Edward D. Lowe, Mark Howarth

How the biotin-streptavidin interaction was made even stronger: investigation via crystallography and a chimeric tetramer

Claire E. CHIVERS*, Apurba L. KONER*, Edward D. LOWE* and Mark HOWARTH*[1]
*Department of Biochemistry, Oxford University, South Parks Road, Oxford, OX1 3QU, UK
[1]To whom correspondence should be addressed (email mark.howarth@bioch.ox.ac.uk).
Department of Biochemistry, Oxford University, South Parks Road, Oxford, OX1 3QU, UK
Telephone: 44-1865-613242
Fax: 44-1865-613201

Synopsis:

The interaction between streptavidin and biotin is one of the strongest non-covalent interactions in nature. Streptavidin is a widely used tool and a paradigm for protein-ligand interactions. We recently developed a streptavidin mutant, termed traptavidin, possessing 10-fold lower off-rate for biotin, with increased mechanical and thermal stability. Here, we determined crystal structures of apo-traptavidin and biotin-traptavidin at 1.5 Å resolution. In apo-streptavidin the L3/4 loop, near biotin's valeryl tail, is typically disordered and open, but closes upon biotin binding. In contrast, this L3/4 loop was shut in both apo-traptavidin and biotin-traptavidin. The reduced flexibility of L3/4 and decreased conformational change on biotin binding provide an explanation for traptavidin's reduced biotin off-rate and on-rate. The L3/4 loop includes Ser-45, which forms a hydrogen bond to biotin consistently in traptavidin but erratically in streptavidin. Reduced breakage of the biotin:Ser-45 hydrogen bond in traptavidin is likely to inhibit the initiating event in biotin's dissociation pathway. We generated a traptavidin with 1 biotin binding site rather than 4, which showed a similarly slow off-rate, demonstrating that traptavidin's slow off-rate was governed by intra-subunit effects. Understanding the structural features of this tenacious interaction may assist design of even stronger affinity tags and inhibitors.

Short title: Traptavidin structure

Keywords: Protein engineering, Avidin, Ultra-stable, Monovalent, High affinity, Femtomolar

Abbreviations used: D, dead streptavidin subunit; L, loop number; rmsd, root mean squared deviation; SA, streptavidin; Tr, traptavidin.

INTRODUCTION

The capture of the small-molecule biotin (vitamin H/ vitamin B_7) by the bacterial protein streptavidin is both a powerful tool in biology and a model system for the study of high-affinity protein-ligand interactions. The key features are the femtomolar affinity, high specificity, fast on-rate and the resilience of streptavidin to pH, temperature and denaturant [1-3]. It is also important that biotin protein ligases can attach biotin to specific lysines *in vitro* or in living cells [4,5]. Streptavidin's applications include imaging [6], nano-assembly [7], and pre-targeted cancer immunotherapy [8]. As a favoured model in biophysics and protein engineering, this protein-ligand interaction has been investigated by at least 200 point mutations of streptavidin [3,9-11], more than 30 alternative small molecule ligands [1,12-14], computational simulation [15-18], crystallography [2], and single-molecule force dynamics [19].

Despite the strength of streptavidin-biotin binding, the interaction can and does fail under challenging conditions. Biotin dissociation becomes significant and sometimes rapid in response to the low pH of the endosomes [20], the high temperatures used for DNA amplification [21], attachment to nanoparticles [22], and shear forces from flow [23]. The slow off-rate of wild-type streptavidin for biotin-conjugates was improved upon recently, when we found that the S52G R53D mutant of streptavidin, named traptavidin, had more than ten-fold slower biotin dissociation than

wild-type streptavidin, as well as enhanced mechanical and thermal stability [24]. The stronger binding of traptavidin enabled us to generate a challenging road-block for one of the fastest known linear molecular motors, FtsK, in order to evaluate the coordination of firing around the hexameric ring as FtsK translocated on DNA [24,25].

To understand the basis of traptavidin's resilient binding and stability to high temperatures, here we solved the crystal structures of both apo-traptavidin and biotin-traptavidin and compared these with existing structures of streptavidin. In addition we purified a monovalent traptavidin, to investigate the role of inter-subunit effects in traptavidin stability and also to characterize a tool which enables ultra-stable binding of biotinylated targets without cross-linking.

EXPERIMENTAL

Traptavidin purification

Traptavidin protein (S52G R53D core streptavidin with a C-terminal His_6 tag, GenBank GU952124) was purified from *Escherichia coli* by inclusion body isolation, refolding, and Ni-NTA chromatography, as described previously [24]. Prior to crystal tray set-up, we performed size-exclusion chromatography (XK 26 column, GE Healthcare), eluting with 50 mM Tris-HCl, 0.5 M NaCl, 10 mM EDTA pH 7.5.

Monovalent traptavidin (Tr1D3) was generated by the mixed refolding of traptavidin (Tr) and dead streptavidin (D) subunits (N23A, S27D, S45A core streptavidin with no His_6 tag). Purification was as previously described for monovalent streptavidin [26], except that the order of SDS-PAGE mobility was reversed (mobility of Tr2D2 >Tr1D3>D4). A tetramer of dead streptavidin subunits (D4) was generated from the refolding of D from inclusion bodies into PBS, and ammonium sulfate precipitation [26].

Apo-traptavidin crystallization

Crystals were obtained by the sitting-drop vapour-diffusion method at 291 K. Apo-traptavidin crystals (space group I 4_1; a = b = 57.59 Å, c = 183.35 Å, with two traptavidin monomers in the asymmetric unit) were obtained from a 4 µl drop of 19 mg/ml solution and a reservoir solution of 12% PEG 8000, 9% ethylene glycol, 0.1 M HEPES pH 7.5. Crystals appeared after 2 days and reached optimum size after 4 days. Prior to data collection, crystals were briefly soaked in a cryoprotectant solution of 12% PEG 8000, 30% ethylene glycol, 0.1 M HEPES pH 7.5 before immersion into liquid nitrogen.

Biotin-traptavidin crystallization

Biotin-bound traptavidin was obtained by incubation of traptavidin with biotin (Acros Organics) in 4-fold molar excess compared to the number of binding sites at 4°C overnight. Biotin-bound crystals (space group P 4_2 2_1 2; a = b = 57.34 Å, c= 77.55 Å, with one monomer in the asymmetric unit) were obtained from a 4 µl drop of 19 mg/ml solution and a reservoir solution of 27% PEG 4000, 0.25 M $MgCl_2$, 0.1 M Tris-HCl pH 8.5. Crystals appeared after 2 days and reached optimum size after 4 days. Prior to data collection, crystals were briefly soaked in a cryoprotectant solution of 27% PEG 4000, 0.25 M $MgCl_2$, 0.1 M Tris-HCl, 25% glycerol pH 8.5 before immersion into liquid nitrogen.

Diffraction data collection

Crystallographic data were collected at 100 K, using an Oxford Cryosystems 700 series Cryostream on an ADSC Quantum 315 CCD detector with an oscillation range of 0.5° at beamline IO2 at the Diamond Light Source, Didcot, UK.

Structure solution and refinement: apo-traptavidin

Data were indexed and integrated using MOSFLM, and scaled and merged using SCALA from the CCP4 program suite [27]. The structure was phased by molecular replacement using a wild-type core-

streptavidin search model (1swb) [28] with the program Phaser. The crystal contained two monomers in the asymmetric unit. Five percent of the reflection data were set aside using the Freerflag program in CCP4 and used for the calculation of R_{free}. The model was built in Coot and refined in PHENIX refine, with incorporation of the twinning operator (-h, k, -l) with a twinning fraction of 49.7%. Throughout the refinement, all data were included from 27.47 Å resolution to the highest limit (1.45 Å) and anisotropic temperature factors were refined. The model was evaluated with MolProbity, which gave Ramachandran statistics with 98% of residues in favoured regions and no outliers. The diffraction-data precision indicator (DPI), indicating the agreement between the model and the x-ray data, for apo-traptavidin was 0.056 Å. The refinement statistics are shown in Table 1.

Structure solution and refinement: biotin-traptavidin

Data were indexed and integrated using MOSFLM, and scaled and merged using SCALA from the CCP4 program suite. Intensities were converted to structure factors using the truncate program in CCP4 and no signs of twinning were observed in the data. The structure was phased by molecular replacement using the apo-traptavidin search model and Phaser. The crystal contained one monomer in the asymmetric unit. Five percent of the reflection data were set aside using the Freerflag program in CCP4 and used for the calculation of R_{free}. Model building was performed in Coot and refinement, including rounds of simulated annealing refinement, in PHENIX refine. Throughout the refinement, all data were included from 38.78 Å resolution to the highest limit (1.49 Å) and anisotropic temperature factors were refined. The presence of a well defined biotin model in the binding pocket was clearly visible in the initial F_{obs}-F_{calc} electron density maps. Biotin coordinates from 1mk5 [29] were used as a template for the refinement and the weighting of coordinate refinement was optimized by PHENIX refine as the refinement progressed. The model was evaluated with MolProbity, which gave Ramachandran statistics with 98% of residues in favoured regions and no outliers. The diffraction-data precision indicator (DPI), indicating the agreement between the model and the x-ray data, for biotin-traptavidin was 0.051 Å. The refinement statistics are shown in Table 1. To assess if model bias was introduced into the biotin-traptavidin model by using the apo-traptavidin structure as a search model for molecular replacement, a simulated annealing composite omit map was calculated using PHENIX AutoBuild [30], with the starting phases provided by the apo-traptavidin structure.

Structure Analysis

Structural overlays and colouring according to B factor were done in PyMOL (DeLano Scientific). Alignments were calculated from main-chain atoms of apo-traptavidin chain A, biotin-traptavidin, apo-streptavidin 1swa, apo-streptavidin 1swb, apo-streptavidin 1swc, and biotin-streptavidin 1swe [28]. Plots of mean B factors of main-chain atoms against residue number were produced using the "baverage" program in CCP4. The diffraction-data precision indicator was assessed using the program SFCHECK from CCP4.

Biotin-conjugate off-rate assay

The off-rate of biotin-4-fluorescein was measured from the fluorescence increase on unbinding at 37 ºC with competing free biotin, as previously [26,31].

Thermostability analysis

3 μM dead streptavidin, tetravalent traptavidin or monovalent traptavidin in PBS was heated at the indicated temperature for 3 min in a DNA Engine® Peltier Thermal Cycler (Bio-Rad). SDS-PAGE to discriminate monomers was performed as described [26]. The band intensities were quantified using a ChemiDoc XRS imager and QuantityOne 4.6 software (Bio-Rad). Percentages were calculated as 100 × (summed intensity of monomer bands at the indicated temperature - summed intensity of monomer bands at 25 ºC) / (summed intensity of monomer bands after 95 ºC with SDS).

RESULTS

Loop L3/4 of traptavidin is closed even without biotin

We determined the crystal structures at high resolution of traptavidin with and without biotin (1.45 Å for apo-traptavidin, PDB 2y3e; 1.49 Å for biotin-traptavidin, PDB 2y3f) (Table 1**)**. Both structures were solved by molecular replacement; the apo-streptavidin structure (1swb) was used as a search model for the apo-traptavidin structure [28]. The subsequent apo-traptavidin structure was used as the search model for biotin-bound traptavidin. To determine whether model bias was introduced into the biotin-traptavidin structure by using the apo-traptavidin structure as a search model for molecular replacement, a simulated annealing composite omit map was calculated. Alignment of this map with the biotin-traptavidin and apo-traptavidin models revealed the final biotin-traptavidin model fitted the omit map much better (correlation coefficient of 0.73 for side-chain atoms) than the apo-traptavidin model (correlation coefficient of 0.47 for side-chain atoms) (Supplementary Figure 1), thus indicating that the solution of the biotin-traptavidin structure was not biased by the search model.

We observed two subunits in the asymmetric unit for apo-traptavidin and one subunit in the asymmetric unit for biotin-traptavidin. We applied symmetry transformations to view the complete tetramer (Figure 1A). Streptavidin/traptavidin subunits are 8-stranded antiparallel β-barrels, with the biotin binding site located at one end of the barrel. Each subunit binds one biotin molecule and the subunits come together to form a tetramer that can be considered a dimer of dimers. The electron density for the biotin bound to traptavidin was unambiguous (Figure 1B). A striking difference between traptavidin and streptavidin was seen in the loop connecting β-strands 3 and 4 (L3/4). The L3/4 loop is commonly disordered in apo-streptavidin ('open' conformation) [28], but becomes ordered on biotin-binding, closing over the binding pocket and forming a 'lid' over the bound biotin ('closed' conformation) (Figure 2A). However, in apo-traptavidin, all the L3/4 loops of the tetramer were already in the 'closed' conformation. The L3/4 loops remained in this closed conformation in biotin-traptavidin (Figure 2A). Apo-streptavidin structures 1swa and 1swb had only one out of four subunits while 1swc had two out of four subunits (1swc) with an ordered L3/4 loop in the tetramer (1swa, 1swb and 1swc have 4 subunits in the asymmetric unit) [28]. We emphasise that the fact that apo-traptavidin had 2 subunits in the asymmetric unit does not mean that the 3rd and 4th subunits were less clearly defined than if there were 4 subunits in the asymmetric unit; rather the crystallographic symmetry tells us that the 3rd and 4th subunits are identical to the 1st and 2nd subunits.

Structural alignments of these apo-streptavidin structures with apo-traptavidin revealed the closed loops in the apo-streptavidin structures are comparable to L3/4 in apo-traptavidin; the root mean squared deviation (rmsd) from apo-traptavidin chain A for residues 45-52 is 0.24 Å for 1swa chain A and 0.20 Å for 1swb chain A. The presence of one 'closed' loop in the apo-streptavidin tetramer suggests that the L3/4 loop is dynamic in the absence of biotin. The L3/4 loop in the 1swc apo-streptavidin structure is an exception, with an alternative open conformation, projecting away from the binding site, and is not comparable to L3/4 in apo-traptavidin (rmsd 2.2 Å compared to 1swc chain B) [28].

The whole structure of traptavidin is pre-formed for biotin binding

Streptavidin does not show cooperativity in biotin binding between the four subunits [32] but there is a substantial conformational change when biotin binds, involving flattening and tighter wrapping of the β-barrels, altered dimer-dimer packing and loop ordering [33]. This conformational change is consistent with an observed increase in thermostability of the biotin-bound tetramer [34]. Upon aligning the apo-traptavidin and biotin-traptavidin structures, we found that the conformational change in traptavidin upon biotin binding is much smaller than for streptavidin (rmsd 0.21 Å for traptavidin, 0.36 Å for streptavidin) (Figure 2B). Differences in the apo- and biotin-bound conformations of streptavidin were clearly shown by calculating alignments of the loops connecting the β-strands (Table 2). It was not just the L3/4 loop which moved less upon biotin binding in traptavidin than streptavidin, but also 5 out of 6 of the other loops.

Changes in the flexibility of traptavidin

To analyze the flexibility and dynamics of apo-traptavidin and biotin-traptavidin, we plotted the mean B factors for main-chain atoms against residue number (Figure 3). Relative B factors within a structure are informative, but it is not straightforward to compare directly the absolute values of B factors between streptavidin and traptavidin, because of different resolutions, data collection conditions and refinement methods.

The B factors for each of the two monomers in the asymmetric unit of apo-traptavidin were plotted to indicate the internal variation. This showed the expected low dynamics in the β-sheet regions and some flexibility in all the loop sections (Figure 3A). The main difference between chains A and B of apo-traptavidin occurs at L5/6 and may result from one chain being involved in crystal contacts at this loop. There is some flexibility in L3/4 for apo-traptavidin but clearly it is less than in apo-streptavidin structures where the loop is not resolved. If L3/4 in apo-traptavidin did not have some flexibility then it is likely that the traptavidin on-rate would be too slow for practical application. The most striking change in the biotin-traptavidin B factors is the loss of flexibility in L3/4, with values comparable to adjacent β-sheets 3 and 4 (Figure 3B), which is consistent with the exceptionally low biotin dissociation rate.

Hydrogen bonding to biotin and Ser-45 in traptavidin and streptavidin

The extensive hydrogen-bonding network from streptavidin to biotin plays a key role in generating the large ΔG°' of biotin binding [2]. We compared all the hydrogen bonds to biotin for traptavidin and streptavidin, paying particular attention to Ser-45 and Asn-49, which are present on the L3/4 loop close to the residues mutated in traptavidin. Factoring in the variation seen in the different chains of the different structures of streptavidin, the hydrogen bonds lengths to biotin are comparable between traptavidin and streptavidin (Supplementary Figure 2).

The published structures of streptavidin allude to the probable dynamic nature of this hydrogen bond network to biotin. In some crystal structures of streptavidin (1swe), each Ser-45 residues has its side-chain hydroxyl directed towards the biotin N3' nitrogen, and hydrogen bonds are formed (although the distance in subunits 1 and 4 in 1swe is at the limit for a hydrogen bond between such atoms, at 3.2 Å) (Figure 4A and Supplementary Figure 2). However, in the streptavidin structure of 1swd, the Ser-45 side-chains point away from the N3' nitrogen and so cannot hydrogen bond (Figure 4A and Supplementary Figure 2). In the traptavidin-biotin structure, the Ser-45 side-chain is clearly orientated towards the N3' nitrogen (Figure 4A), with a hydrogen bond length of 3.0 Å. Gly-52 in traptavidin undergoes little change upon biotin binding (Figure 4B). The peculiar importance of the S52G mutation for biotin binding stability is likely to relate to Ser-52 stabilizing an alternative open conformation of L3/4, thereby destabilizing the Ser-45 hydrogen bond to biotin. In this rival conformation, Ser-52's main-chain carbonyl forms a hydrogen bond to the main-chain N-H of Ser-45, while the Ser-52 side-chain makes a hydrogen-bond to the main-chain N-H of Ala-46 (Figure 4B). This competing pairing is seen in apo-streptavidin structures with an undefined L3/4 loop (1swa) [28], but could well form transiently even in the presence of biotin, so contributing to the rare biotin dissociation events from streptavidin.

The network of polar and non-polar interactions made to biotin by streptavidin changes biotin's structure from the conformation reported to apply in solution [35]. In avidin and streptavidin there are 3 residues which are positioned to hydrogen bond to the carbonyl oxygen of biotin, suggesting that this oxygen is partially charged and that this polarization may contribute to the exceptional affinity of biotin binding [16]. The bond lengths and bond angles of biotin were similar between streptavidin and traptavidin (data not shown), indicating that changes in biotin's electronic structure in the binding site are not likely to contribute to the difference in biotin off-rate.

Generating monovalent traptavidin shows that altered intersubunit contacts do not explain traptavidin's increased stability

We created tetramers with exactly one traptavidin subunit and three "dead" subunits which do not bind biotin [26], to give monovalent traptavidin (Tr1D3) (Figure 5A). We previously showed that monovalent streptavidin had equivalent biotin binding stability to tetravalent streptavidin [26]. Here we used monovalent traptavidin to explore whether the increased stability of wild-type traptavidin

(Tr4) over streptavidin depended upon the presence of neighbouring traptavidin subunits. The off-rate of biotin-4-fluorescein was compared for tetravalent traptavidin, monovalent traptavidin and tetravalent streptavidin (Figure 5B). Monovalent traptavidin had equivalent off-rate to tetravalent traptavidin, showing that it is the binding by the traptavidin subunit and not any altered intersubunit interaction that is the dominant factor in traptavidin's improved biotin binding stability.

Traptavidin stays tetrameric and remains bound to biotin-conjugates at higher temperatures than streptavidin [24]. We tested the thermostability of monovalent traptavidin by incubating at a range of temperatures and testing by SDS-PAGE what fraction remained tetrameric (Figure 5C). Monovalent streptavidin is known to show equivalent thermostability to wild-type streptavidin [26]. We compared monovalent traptavidin to tetravalent traptavidin and a tetramer composed entirely of dead subunits (D4). Tetravalent traptavidin was ~10ºC more stable than the dead tetramer. The thermostability of monovalent traptavidin was similar to D4, consistent with the least stable subunit dominating the stability of the tetramer.

DISCUSSION

Streptavidin's binding to biotin is one of the strongest known non-covalent protein-ligand interactions and yet the mutant protein traptavidin has 10-fold greater binding stability [24]. The crystal structures of apo- and biotin-bound traptavidin described here show the basis for traptavidin's tenacious ligand binding. The key differences between traptavidin and streptavidin are the decreased flexibility of the L3/4 loop, the increased stability of the Ser-45 hydrogen bond to biotin, and the reduced conformational change upon biotin binding.

The crystal structure of D128A streptavidin and molecular dynamic simulations [15,36,37] led to a model whereby a water molecule initiates biotin dissociation, by competing with the Asp-128 hydrogen bond to biotin and so promoting cooperative breakage of other biotin hydrogen bonds. However, we note that in wild-type streptavidin the Asp-128 hydrogen bond to biotin is always in place, but the Ser-45 hydrogen bond is often broken [28]. Hence we suggest that breakage of the Ser-45 hydrogen bond to biotin is frequent and is the first event in biotin dissociation. The mutations that led to a higher stability mutant, traptavidin, further support this revised model: in traptavidin, the Ser-45 hydrogen bond to biotin was clearly present, while the residue that competes with biotin for hydrogen bonding to Ser-45, Ser-52, is mutated to Gly. Arg-53 does not have direct interactions with residues binding to biotin, so the R53D mutation is likely to exert its effects by further reducing L3/4 loop mobility.

The L3/4 loop is always in a 'closed' conformation in biotin-bound structures of streptavidin, acting like a lid over the binding pocket and contributing to the low rate of biotin dissociation. For avidin, the L3/4 loop is ordered when bound to *free biotin*, but disordered when bound to *biotin-conjugates*: this explains why avidin binds biotin-conjugates much more weakly than biotin [38]. A restrained L3/4 loop may also be important in enabling high affinity biotin binding by the dimeric rhizavidin [39]. In a series of structures solved in the pH range 2.0-3.1 [40], the L3/4 loop was closed in apo-streptavidin, but in the apo-streptavidin structures solved in the more physiologically relevant pH range 4.5-7.5, the L3/4 loop is disordered, in two (1swc) or three (1swa and 1swb) of the subunits of the tetramer [28]. The stability of the L3/4 loop in the closed conformation in apo-traptavidin indicates that in biotin-traptavidin the occasional fluctuations that lead to lid opening and so facilitate biotin dissociation are similarly suppressed. Since we found that the hydrogen bond lengths to biotin and conformation of biotin are equivalent in traptavidin and streptavidin, this indicates that it is not subtle differences in the ground-state binding conformation that explain the change in stability, but a change in the frequency of alternative protein conformations with weakened binding. The L3/4 loop conformation in apo-traptavidin also rationalizes the decreased on-rate of traptavidin [24], since it will be harder for biotin to enter the binding site with the loop shut. For *Streptomyces avidinii*, one can hypothesize that evolution would favour a streptavidin with a fast on-rate as well as a slow off-rate, but for laboratory applications in anchoring and bridging [24] the off-rate is more important.

Streptavidin is a highly thermostable protein (72 ºC for subunit dissociation without biotin), even though the protein derives from a mesophilic bacterium [1,2,34]. This thermostability relates to reducing the rare subunit unfolding events that would contribute to ligand dissociation, or, from an energetic perspective, rigid binding sites having a reduced entropic cost for providing an inflexible

ligand binding site [41]. Any fleeting disruption of the interaction between biotin and Trp-120 of the neighbouring subunit should transiently increase the rate of biotin dissociation 10^4-fold [42]. Traptavidin is 10 ºC more thermostable than streptavidin [24] and one might think that this thermostability would contribute to the increased ligand binding stability, by further reducing the frequency of conformational fluctuations that disrupt the protein structure or subunit packing. The equivalent off-rate of monovalent and tetravalent traptavidin demonstrated that the change in traptavidin's biotin binding stability is not mediated through altered subunit interactions. The tetravalent nature of traptavidin interferes with many applications: for example in imaging cell-surface proteins, tetravalency can induce receptor cross-linking and activate cell signaling [6,26]. Monovalent traptavidin (and divalent or trivalent traptavidin, which could be generated, as before [26]) should be valuable in diverse applications, including nanoassembly and the targeting of quantum dots for photostable single-molecule imaging [5,6].

The stability of the interaction between biotin and avidin/streptavidin is paradoxical, given the known binding energy that can be obtained from a given number of hydrogen-bonds and from a given surface area, allowing hydrophobic and van der Waals interactions [43,44]. The mutations that generated a higher stability variant of streptavidin were in the second shell of residues around biotin, pointing to the difficulty of optimizing this kind of high affinity interaction computationally. Although we have sufficient knowledge to enable computational and structure-guided design of protein-ligand interactions with micromolar and sometimes nanomolar affinity [44-46], the factors responsible for increasing affinity into the picomolar and femtomolar range are still enigmatic [47,48]. Hydrogen/deuterium exchange mass spectrometry, now possible with single residue resolution, may be able to build upon our crystal structures for further enlightenment on the "perfect storm" of molecular events required for biotin to overcome the large activation barrier to dissociate from traptavidin [49]. As well as suggesting how to improve further the applications of biotin as an affinity tag, the structures of traptavidin shed light on the origins of extreme-affinity interactions, with implications for the rational design of drugs with improved efficacy.

ACKNOWLEDGEMENTS

We thank Sonja Baumli for assistance in crystal freezing. Traptavidin is subject to a UK priority patent application (0919102.4) filed on 30th October 2009.

FUNDING

Funding was provided by the Wellcome Trust (A.L.K. and M.H.), the Biotechnology and Biological Sciences Research Council (C.E.C.), Oxford University (E.D.L.), and Worcester College Oxford (M.H.).

REFERENCES

1 Sano, T., Vajda, S. and Cantor, C. R. (1998) Genetic engineering of streptavidin, a versatile affinity tag. J. Chromatogr. B Biomed. Sci. Appl., **715,** 85-91.
2 Stayton, P. S., Freitag, S., Klumb, L. A., Chilkoti, A., Chu, V., Penzotti, J. E., To, R., Hyre, D., Le Trong, I., Lybrand, T. P. and Stenkamp, R. E. (1999) Streptavidin-biotin binding energetics. Biomol. Eng, **16,** 39-44.
3 Laitinen, O. H., Hytonen, V. P., Nordlund, H. R. and Kulomaa, M. S. (2006) Genetically engineered avidins and streptavidins. Cell Mol. Life Sci., **63,** 2992-3017.
4 de Boer, E., Rodriguez, P., Bonte, E., Krijgsveld, J., Katsantoni, E., Heck, A., Grosveld, F. and Strouboulis, J. (2003) Efficient biotinylation and single-step purification of tagged transcription factors in mammalian cells and transgenic mice. Proc. Natl. Acad. Sci. U. S. A, **100,** 7480-7485.
5 Howarth, M., Takao, K., Hayashi, Y. and Ting, A. Y. (2005) Targeting quantum dots to surface proteins in living cells with biotin ligase. Proc. Natl. Acad. Sci. U. S. A, **102,** 7583-7588.
6 Howarth, M., Liu, W., Puthenveetil, S., Zheng, Y., Marshall, L. F., Schmidt, M. M., Wittrup, K. D., Bawendi, M. and Ting, A. Y. (2008) Monovalent, reduced-size quantum dots for single molecule imaging of receptors in living cells. Nat. Methods, **5,** 397-399.
7 Kattah, M. G., Coller, J., Cheung, R. K., Oshidary, N. and Utz, P. J. (2008) HIT: a versatile proteomics platform for multianalyte phenotyping of cytokines, intracellular proteins and surface molecules. Nat. Med., **14,** 1284-1289.
8 Goldenberg, D. M., Sharkey, R. M., Paganelli, G., Barbet, J. and Chatal, J. F. (2006) Antibody pretargeting advances cancer radioimmunodetection and radioimmunotherapy. J. Clin. Oncol., **24,** 823-834.
9 Avrantinis, S. K., Stafford, R. L., Tian, X. and Weiss, G. A. (2002) Dissecting the streptavidin-biotin interaction by phage-displayed shotgun scanning. Chembiochem., **3,** 1229-1234.
10 Aslan, F. M., Yu, Y., Mohr, S. C. and Cantor, C. R. (2005) Engineered single-chain dimeric streptavidins with an unexpected strong preference for biotin-4-fluorescein. Proc. Natl. Acad. Sci. U. S. A, **102,** 8507-8512.
11 Levy, M. and Ellington, A. D. (2008) Directed evolution of streptavidin variants using in vitro compartmentalization. Chem. Biol., **15,** 979-989.
12 Green, N. M. (1975) Avidin. Adv. Protein Chem., **29,** 85-133.
13 Wilbur, D. S., Pathare, P. M., Hamlin, D. K., Stayton, P. S., To, R., Klumb, L. A., Buhler, K. R. and Vessella, R. L. (1999) Development of new biotin/streptavidin reagents for pretargeting. Biomol. Eng, **16,** 113-118.
14 Weber, P. C., Pantoliano, M. W., Simons, D. M. and Salemme, F. R. (1994) Structure-Based Design of Synthetic Azobenzene Ligands for Streptavidin. Journal of the American Chemical Society, **116,** 2717-2724.
15 Grubmuller, H., Heymann, B. and Tavan, P. (1996) Ligand binding: molecular mechanics calculation of the streptavidin-biotin rupture force. Science, **271,** 997-999.
16 DeChancie, J. and Houk, K. N. (2007) The origins of femtomolar protein-ligand binding: hydrogen-bond cooperativity and desolvation energetics in the biotin-(strept)avidin binding site. J. Am. Chem. Soc., **129,** 5419-5429.
17 Cerutti, D. S., Le, T., I, Stenkamp, R. E. and Lybrand, T. P. (2009) Dynamics of the streptavidin-biotin complex in solution and in its crystal lattice: distinct behavior revealed by molecular simulations. J. Phys. Chem. B, **113,** 6971-6985.
18 Miyamoto, S. and Kollman, P. A. (1993) Absolute and relative binding free energy calculations of the interaction of biotin and its analogs with streptavidin using molecular dynamics/free energy perturbation approaches. Proteins, **16,** 226-245.
19 Moy, V. T., Florin, E. L. and Gaub, H. E. (1994) Intermolecular forces and energies between ligands and receptors. Science, **266,** 257-259.
20 Bruneau, E., Sutter, D., Hume, R. I. and Akaaboune, M. (2005) Identification of nicotinic acetylcholine receptor recycling and its role in maintaining receptor density at the neuromuscular junction in vivo. J. Neurosci., **25,** 9949-9959.

21 Dressman, D., Yan, H., Traverso, G., Kinzler, K. W. and Vogelstein, B. (2003) Transforming single DNA molecules into fluorescent magnetic particles for detection and enumeration of genetic variations. Proc. Natl. Acad. Sci. U. S. A, **100,** 8817-8822.
22 Swift, J. L., Heuff, R. and Cramb, D. T. (2006) A two-photon excitation fluorescence cross-correlation assay for a model ligand-receptor binding system using quantum dots. Biophys. J., **90,** 1396-1410.
23 Pierres, A., Touchard, D., Benoliel, A. M. and Bongrand, P. (2002) Dissecting streptavidin-biotin interaction with a laminar flow chamber. Biophys. J., **82,** 3214-3223.
24 Chivers, C. E., Crozat, E., Chu, C., Moy, V. T., Sherratt, D. J. and Howarth, M. (2010) A streptavidin variant with slower biotin dissociation and increased mechanostability. Nat. Methods, **7,** 391-393.
25 Crozat, E., Meglio, A., Allemand, J. F., Chivers, C. E., Howarth, M., Venien-Bryan, C., Grainge, I. and Sherratt, D. J. (2010) Separating speed and ability to displace roadblocks during DNA translocation by FtsK. EMBO J., **29,** 1423-1433.
26 Howarth, M., Chinnapen, D. J., Gerrow, K., Dorrestein, P. C., Grandy, M. R., Kelleher, N. L., El Husseini, A. and Ting, A. Y. (2006) A monovalent streptavidin with a single femtomolar biotin binding site. Nat. Methods, **3,** 267-273.
27 Collaborative Computational Project Number 4. (1994) The CCP4 suite: programs for protein crystallography. Acta Crystallogr. D. Biol. Crystallogr., **50,** 760-763.
28 Freitag, S., Le Trong, I., Klumb, L., Stayton, P. S. and Stenkamp, R. E. (1997) Structural studies of the streptavidin binding loop. Protein Sci., **6,** 1157-1166.
29 Hyre, D. E., Le Trong, I., Merritt, E. A., Eccleston, J. F., Green, N. M., Stenkamp, R. E. and Stayton, P. S. (2006) Cooperative hydrogen bond interactions in the streptavidin-biotin system. Protein Sci., **15,** 459-467.
30 Terwilliger, T. C., Grosse-Kunstleve, R. W., Afonine, P. V., Moriarty, N. W., Zwart, P. H., Hung, L. W., Read, R. J. and Adams, P. D. (2008) Iterative model building, structure refinement and density modification with the PHENIX AutoBuild wizard. Acta Crystallogr. D. Biol. Crystallogr., **64,** 61-69.
31 Kada, G., Falk, H. and Gruber, H. J. (1999) Accurate measurement of avidin and streptavidin in crude biofluids with a new, optimized biotin-fluorescein conjugate. Biochim. Biophys. Acta, **1427,** 33-43.
32 Jones, M. L. and Kurzban, G. P. (1995) Noncooperativity of biotin binding to tetrameric streptavidin. Biochemistry, **34,** 11750-11756.
33 Weber, P. C., Ohlendorf, D. H., Wendoloski, J. J. and Salemme, F. R. (1989) Structural origins of high-affinity biotin binding to streptavidin. Science, **243,** 85-88.
34 Bayer, E. A., Ehrlich-Rogozinski, S. and Wilchek, M. (1996) Sodium dodecyl sulfate-polyacrylamide gel electrophoretic method for assessing the quaternary state and comparative thermostability of avidin and streptavidin. Electrophoresis, **17,** 1319-1324.
35 Li, Q., Gusarov, S., Evoy, S. and Kovalenko, A. (2009) Electronic structure, binding energy, and solvation structure of the streptavidin-biotin supramolecular complex: ONIOM and 3D-RISM study. J. Phys. Chem. B, **113,** 9958-9967.
36 Freitag, S., Chu, V., Penzotti, J. E., Klumb, L. A., To, R., Hyre, D., Le Trong, I., Lybrand, T. P., Stenkamp, R. E. and Stayton, P. S. (1999) A structural snapshot of an intermediate on the streptavidin-biotin dissociation pathway. Proc. Natl. Acad. Sci. U. S. A, **96,** 8384-8389.
37 Hyre, D. E., Amon, L. M., Penzotti, J. E., Le Trong, I., Stenkamp, R. E., Lybrand, T. P. and Stayton, P. S. (2002) Early mechanistic events in biotin dissociation from streptavidin. Nat. Struct. Biol., **9,** 582-585.
38 Pazy, Y., Kulik, T., Bayer, E. A., Wilchek, M. and Livnah, O. (2002) Ligand exchange between proteins. Exchange of biotin and biotin derivatives between avidin and streptavidin. J. Biol. Chem., **277,** 30892-30900.
39 Meir, A., Helppolainen, S. H., Podoly, E., Nordlund, H. R., Hytonen, V. P., Maatta, J. A., Wilchek, M., Bayer, E. A., Kulomaa, M. S. and Livnah, O. (2009) Crystal structure of rhizavidin: insights into the enigmatic high-affinity interaction of an innate biotin-binding protein dimer. J. Mol. Biol., **386,** 379-390.
40 Katz, B. A. (1997) Binding of biotin to streptavidin stabilizes intersubunit salt bridges between Asp61 and His87 at low pH. J. Mol. Biol., **274,** 776-800.

41 Moghaddam, S., Inoue, Y. and Gilson, M. K. (2009) Host-guest complexes with protein-ligand-like affinities: computational analysis and design. J. Am. Chem. Soc., **131,** 4012-4021.
42 Chilkoti, A., Tan, P. H. and Stayton, P. S. (1995) Site-directed mutagenesis studies of the high-affinity streptavidin-biotin complex: contributions of tryptophan residues 79, 108, and 120. Proc. Natl. Acad. Sci. U. S. A, **92,** 1754-1758.
43 Kuntz, I. D., Chen, K., Sharp, K. A. and Kollman, P. A. (1999) The maximal affinity of ligands. Proc. Natl. Acad. Sci. U. S. A, **96,** 9997-10002.
44 Houk, K. N., Leach, A. G., Kim, S. P. and Zhang, X. (2003) Binding affinities of host-guest, protein-ligand, and protein-transition-state complexes. Angew. Chem. Int. Ed Engl., **42,** 4872-4897.
45 Das, R. and Baker, D. (2008) Macromolecular modeling with rosetta. Annu. Rev. Biochem., **77,** 363-382.
46 Holm, L., Moody, P. and Howarth, M. (2009) Electrophilic affibodies forming covalent bonds to protein targets. J. Biol. Chem., **284,** 32906-32913.
47 Midelfort, K. S., Hernandez, H. H., Lippow, S. M., Tidor, B., Drennan, C. L. and Wittrup, K. D. (2004) Substantial energetic improvement with minimal structural perturbation in a high affinity mutant antibody. J. Mol. Biol., **343,** 685-701.
48 Foote, J. and Eisen, H. N. (2000) Breaking the affinity ceiling for antibodies and T cell receptors. Proc. Natl. Acad. Sci. U. S. A, **97,** 10679-10681.
49 Rand, K. D., Zehl, M., Jensen, O. N. and Jorgensen, T. J. (2009) Protein hydrogen exchange measured at single-residue resolution by electron transfer dissociation mass spectrometry. Anal. Chem., **81,** 5577-5584.

TABLES

Table 1 Data collection and refinement statistics for crystal structures of apo-traptavidin and biotin-traptavidin

Values in parentheses are for the highest-resolution shell.

	Apo-traptavidin (PDB 2y3e)	**Biotin-traptavidin** (PDB 2y3f)
DATA COLLECTION		
Space group	*I* 4_1	*P* 4_2 2_1 2
Cell dimensions		
a, *b*, *c* (Å)	57.59, 57.59, 183.35	57.34, 57.34, 77.55
α, β, γ (°)	90.00, 90.00, 90.00	90.00, 90.00, 90.00
Resolution (Å)	27.47 - 1.45 (1.53 - 1.45)	38.78 - 1.49 (1.57 - 1.49)
R_{merge}	0.052 (0.619)	0.069 (0.085)
$I / \sigma I$	13.6 (2.0)	26.0 (19.6)
Completeness (%)	97.8 (87.1)	100.0 (100.0)
Multiplicity	3.6 (3.2)	7.0 (7.1)
REFINEMENT		
Resolution (Å)	27.47 - 1.45	32.12 - 1.49
No. reflections	48,884	21,581
R_{work} / R_{free}	0.134 / 0.178	0.135 / 0.152
No. atoms		
Protein	1,855	954
Biotin	n/a	16
Glycerol	18	18
Water	321	142
B factors (mean of all atoms, Å^2)		
Protein	33.41	10.10
Biotin	n/a	5.83
Glycerol	44.14	28.31
Water	38.19	27.92
Rmsd		
Bond length rmsd (Å)	0.005	0.009
Bond angle rmsd (°)	0.93	1.48
Twinning		
Twin operator	-h, k, -l	n/a
Twin fraction	0.497	n/a

Biochemical Journal Immediate Publication. Published on 18 Jan 2011 as manuscript BJ20101593

Table 2 Structural alignments of loop regions

(**A**) Loops of apo-traptavidin were aligned to biotin-traptavidin and apo/biotin-streptavidin. Residues comprising each loop are shown in parentheses. (**B**) Loops of apo-streptavidin were aligned to biotin-streptavidin and apo/biotin-traptavidin. Only main-chain atoms were used to calculate the alignments. *The loop of 1swa was compared only for the resolved residues of 45 and 49-52, since 46-48 were disordered.

A

	Rmsd (Å) of alignment of loop in:		
Apo-traptavidin (chain A) aligned with:	Biotin-traptavidin	Apo-streptavidin (1swa chain B)	Biotin-streptavidin (1swe chain D)
L1/2 (23-26)	0.050	0.20	0.21
L2/3 (33-38)	0.14	0.23	0.15
L3/4 (45-52)	0.25	2.3*	0.25
L4/5 (62-70)	0.20	0.20	0.22
L5/6 (79-88)	0.18	0.28	0.18
L6/7 (98-102)	0.14	0.22	0.37
L7/8 (113-121)	0.20	0.23	0.24
Overall structure	0.21	0.29	0.35

B

	Rmsd (Å) of alignment of loop in:		
Apo-streptavidin (1swa chain B) aligned with:	Biotin-streptavidin (1swe, chain D)	Apo-traptavidin (chain A)	Biotin-traptavidin
L1/2 (23-26)	0.27	0.20	0.18
L2/3 (33-38)	0.23	0.23	0.22
L3/4 (45-52)	2.6*	2.3*	2.3*
L4/5 (62-70)	0.25	0.20	0.25
L5/6 (79-88)	0.31	0.28	0.27
L6/7 (98-102)	0.42	0.22	0.26
L7/8 (113-121)	0.17	0.23	0.15
Overall structure	0.36	0.29	0.25

FIGURE LEGENDS

Figure 1 Crystal structures of traptavidin

(**A**) Structure of the complete tetramers of apo-traptavidin (left) and biotin-traptavidin (right), with each subunit of the tetramer in a different colour. Biotin bound to each subunit is shown in space-filling mode. (**B**) F_{obs}-F_{calc} map of the biotin binding pocket in biotin-traptavidin, showing the electron density for biotin, with the protein overlaid in cartoon format. The L3/4 loop is shown in red and the residues mutated in traptavidin in stick format.

Figure 2 The L3/4 loop of traptavidin is shut with and without biotin

(**A**) Comparison of the structure of individual subunits of traptavidin or streptavidin, with or without biotin. Traptavidin (top row) has a well-defined closed L3/4 loop (coloured red) in both apo- (left) and biotin-bound structures (right). For streptavidin (bottom row) the L3/4 loop is disordered in apo-streptavidin (left) (1swa chain B) but ordered in biotin-streptavidin (1swe chain D) (right) [28]. Biotin is shown in space-filling mode. (**B**) Conformation changes on biotin binding in traptavidin (left) and streptavidin (right), shown as individual subunits. The apo-structure in green is overlaid with the biotin-bound structure in blue.

Figure 3 Traptavidin flexibility

(**A**) B factors (indicating dynamics and flexibility) averaged over main-chain atoms for each amino acid residue are plotted for apo-traptavidin, with the two chains of the asymmetric unit shown separately. Regions corresponding to loops are labeled L. (**B**) Mean main-chain B factors for each residue of biotin-traptavidin, with loops labeled. (C) Heat map showing mean main-chain B factors for an individual subunit of apo-traptavidin (left, chain A) or biotin-traptavidin (right), with biotin shown in space-filling mode. Red indicates the most flexible and blue the least flexible region of the particular subunit.

Figure 4 Hydrogen bonding by Ser-45 in traptavidin

(**A**) The electron density for biotin and Ser-45 surrounds a stick model of the atoms involved, for traptavidin (left), and two different streptavidin structures (1swd in the middle and 1swe on the right). Hydrogen bonds are indicated by a dotted line. (**B**) The rival hydrogen bonding by Ser-45. An overlay of the L3/4 loop region, with key residues highlighted in stick format. For traptavidin (left panel) with and without biotin the L3/4 loop is closed, with no hydrogen bond between Ser-45 and Gly-52. For streptavidin (right panel) without biotin and with an undefined L3/4 loop (1swa, chain B), Ser-52 forms hydrogen bonds to Ser-45 and Ala-46 (indicated by dotted lines). When biotin is bound and the loop is closed (1swe, chain D), Ser-45 now forms a hydrogen-bond to biotin.

Figure 5 Monovalent traptavidin off-rate and thermostability

(**A**) The traptavidin tetramer (left, Tr4) is tetravalent, with each subunit binding one biotin (b). Monovalent traptavidin contains one traptavidin subunit (Tr, white square) and three dead subunits (D, grey squares) which cannot bind biotin. Tr but not D subunits have His_6 tags (black diagonal line). (**B**) Off-rate of a biotin-conjugate from monovalent traptavidin (Tr1D3), compared to tetravalent streptavidin (SA) and tetravalent traptavidin (Tr4) in the presence of competing free biotin at 37 ºC. Means of triplicate readings are shown ± 1 S.D. (**C**) Thermostability of the monovalent traptavidin tetramer, incubated at the indicated temperature for 3 min and analyzed by SDS-PAGE and Coomassie staining. The positive control (c) was mixed with SDS before heating at 95 ºC. Bands from tetrameric Tr1D3 or monomers (Tr or D) are indicated. The percentage monomer of monovalent traptavidin from duplicate gels (adjacent striped columns) is plotted against temperature in the lower panel, with comparison to either a tetravalent traptavidin (Tr4, white columns) or a tetramer of dead subunits (D4, filled columns).

Figure 1

A

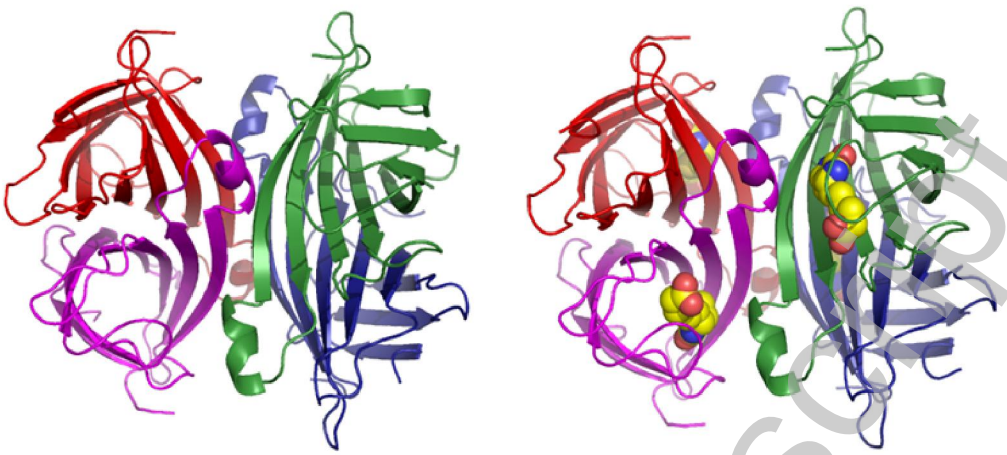

Apo-traptavidin Biotin-traptavidin

B

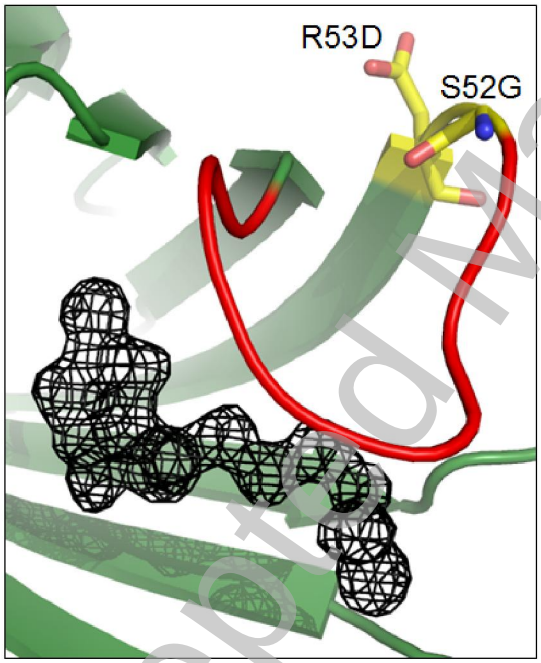

Figure 2

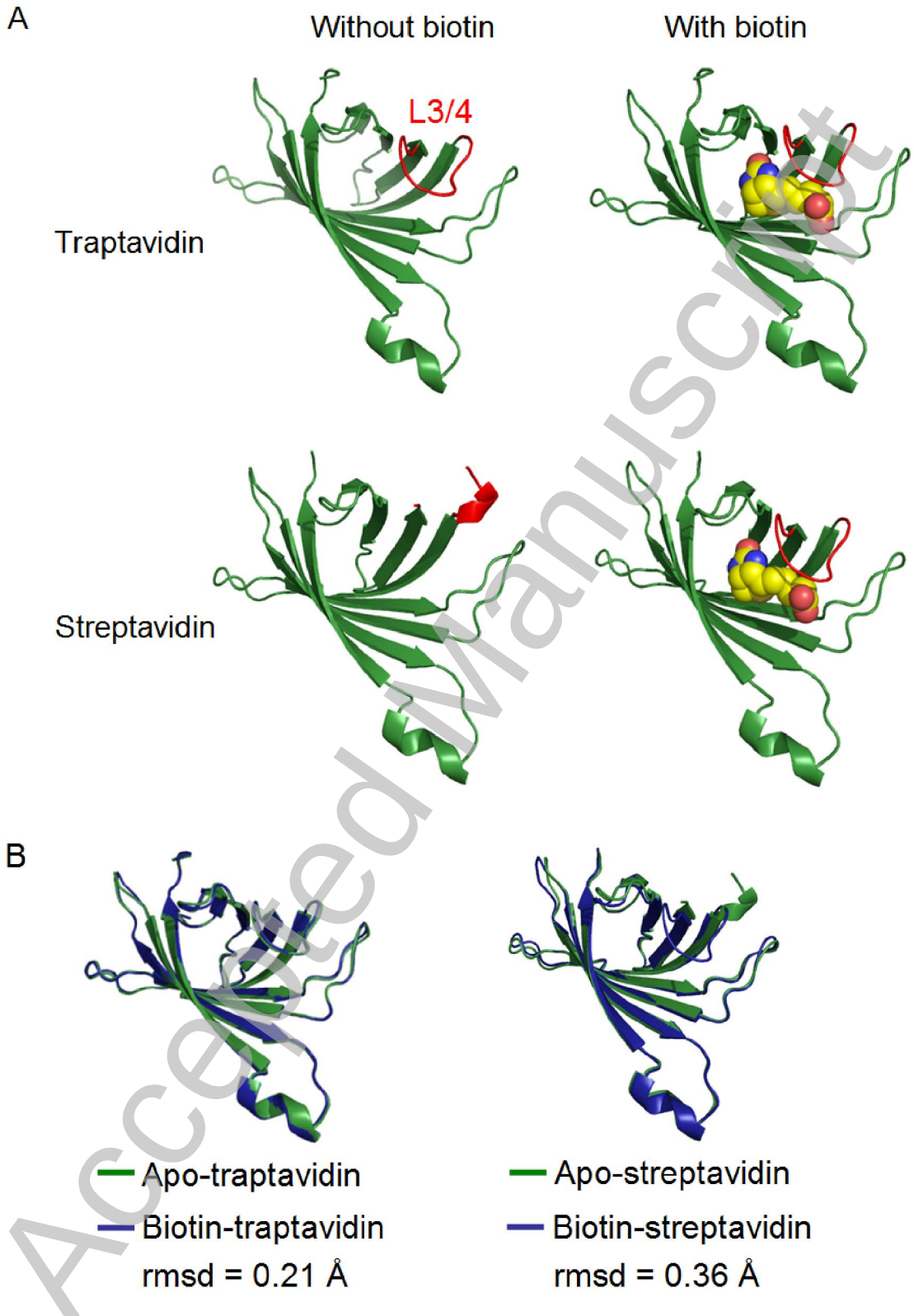

Figure 3

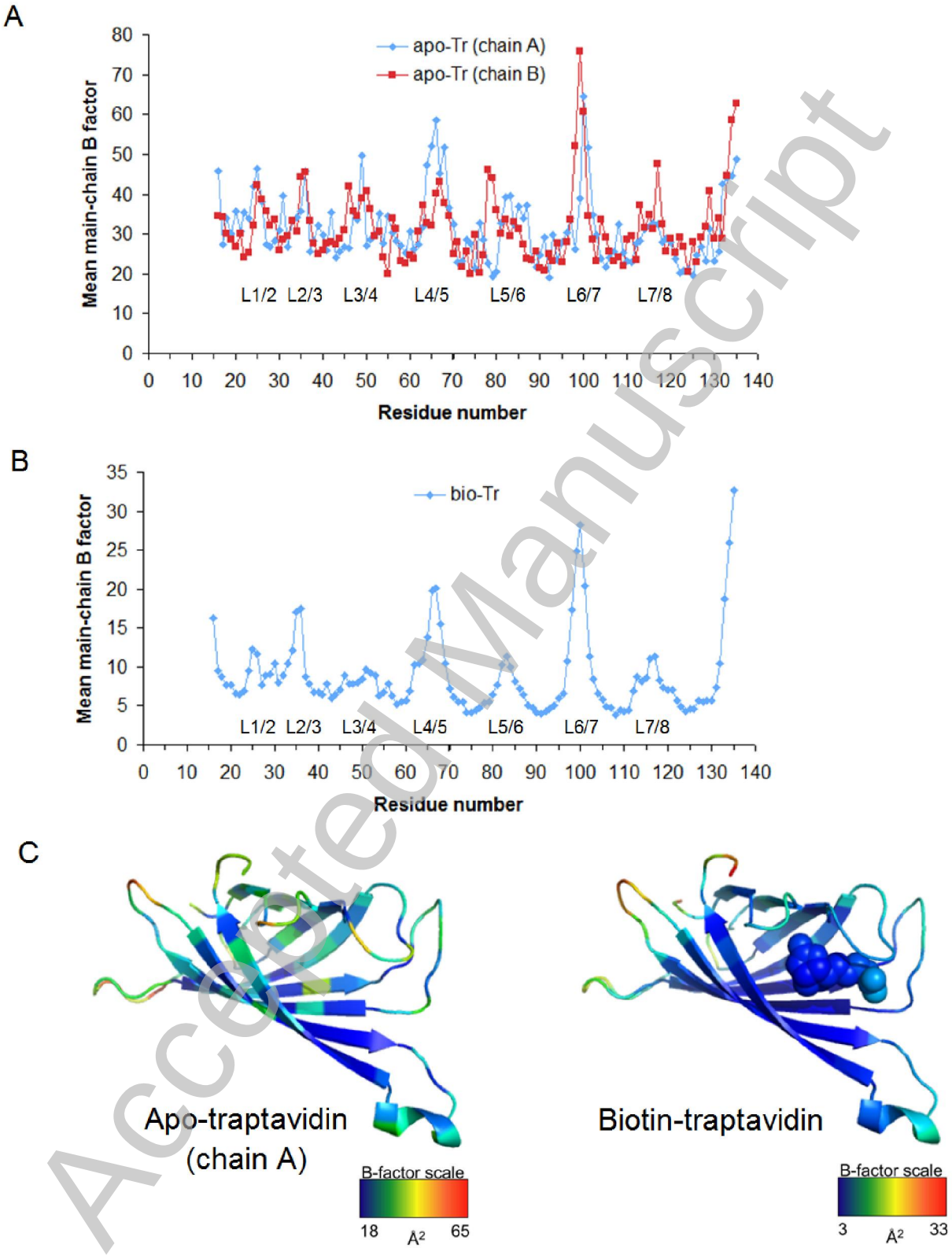

Figure 4

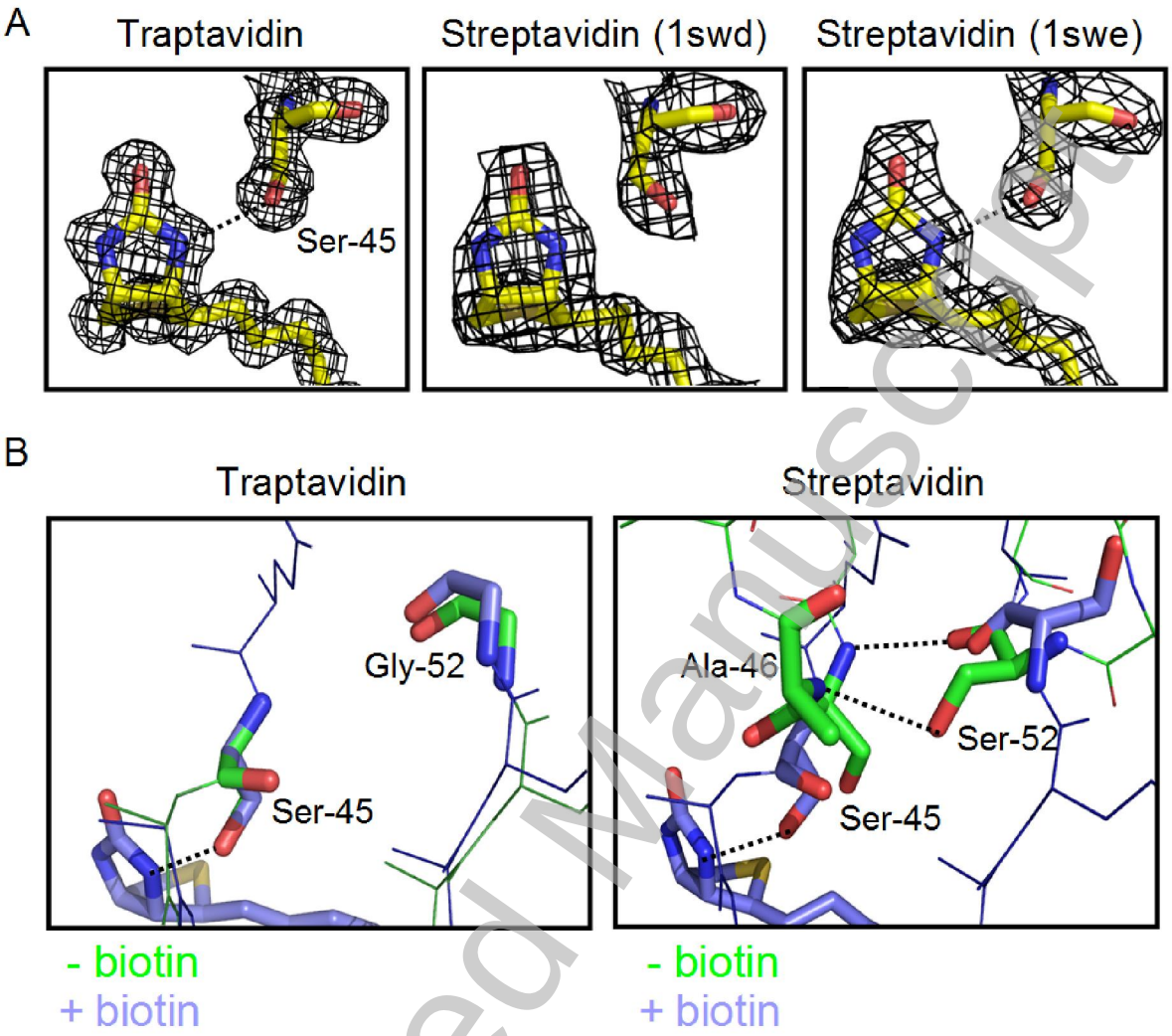

Figure 5